APPLICATIONS OF RANDOM FIELD MODELS IN STOCHASTIC STRUCTURAL MECHANICS

Christian Bucher
Institute of Structural Mechanics,
Bauhaus-University Weimar, Germany

Abstract

Stochastic structural mechanics deals with the analysis of random phenomena occurring in structural systems or components. There are two major categories of structural uncertainties which involve spatial correlation and which consequently require the treatment as random fields. These are:

- Material properties such as modulus of elasticity or strength,
- Geometrical properties such as shape or thickness

of structural components. The outcome of the stochastic structural analyses is significantly affected by the appropriate treatment of the random properties in the context of the Finite Element method.

The paper will provide an overview of random field representation as appropriate for the stochastic finite element method (cf. Matthies and Bucher, 1999). This includes integral representation models as well a point representation models. In addition, conditional random fields as required in the presence of pointwise deterministic information (e.g. from measurements) are introduced.

Example applications illustrate these concepts and discuss the numerical implications of random field modeling. These applications involve static and dynamic problems which arise in system identification (Macke and Bucher, 2000; Bucher et al., 2003) as well as dynamic stability issues due to geometrical imperfections of shells (Most et al., 2004).

1. Random Fields

A *random field* $H(\mathbf{x})$ is a real-valued random variable whose statistics (mean value, standard deviation, etc.) may be different for each value of $\mathbf{x}$ (Matthies et al., 1997; Matthies and Bucher, 1999), i.e.,

$$H \in \mathbb{R}; \quad \mathbf{x} = [x_1, x_2, \ldots x_n]^T \in \mathcal{D} \subset \mathbb{R}^n. \tag{1}$$

The *mean value function* is defined as

$$\bar{H}(\mathbf{x}) = \mathbf{E}[H(\mathbf{x})], \tag{2}$$

whereby the expectation operator $\mathbf{E}$ is to be taken at a fixed location $\mathbf{x}$ across the ensemble, i.e., over all possible realizations $H(\mathbf{x}, \omega)$ of the random field (see Figure 1).

The spatial correlation, i.e., the fact that we observe a specific dependency structure of random field values $H(\mathbf{x})$ and $H(\mathbf{y})$ taken at different locations $\mathbf{x}$ and $\mathbf{y}$ is described by the *auto-covariance function*

$$C_{HH}(\mathbf{x}, \mathbf{y}) = \mathbf{E}[\{H(\mathbf{x}) - \bar{H}(\mathbf{x})\}\{H(\mathbf{y}) - \bar{H}(\mathbf{y})\}]. \tag{3}$$

With respect to the form of the auto-covariance function we can classify the random fields. A random field $H(\mathbf{x})$ is called *weakly homogeneous* if

$$\bar{H}(\mathbf{x}) = \text{const.} \quad \forall \mathbf{x} \in \mathcal{D}; \quad C_{HH}(\mathbf{x}, \mathbf{x} + \boldsymbol{\xi}) = C_{HH}(\boldsymbol{\xi}) \quad \forall \mathbf{x} \in \mathcal{D}. \tag{4}$$

M. Pandey et al. (eds), Advances in Engineering Structures, Mechanics & Construction, 471–484.

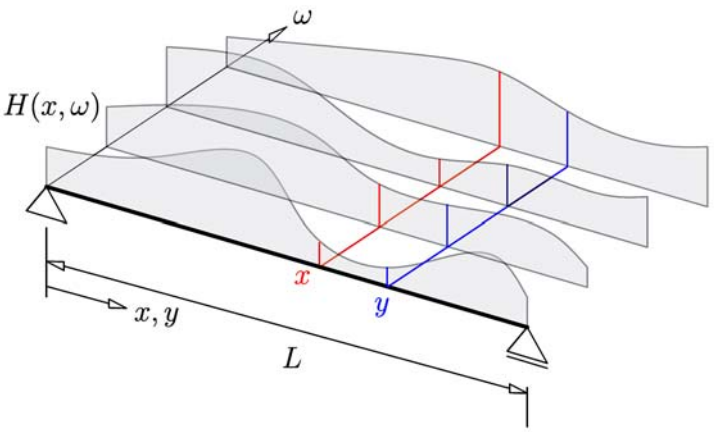

Fig. 1. Ensemble of realizations of one-dimensional random field.

This property is equivalent to the stationarity of a random process. If the covariance function depends on the distance only (not on the direction), i.e.,

$$C_{HH}(\mathbf{x}, \mathbf{x}+\boldsymbol{\xi}) = C_{HH}(\|\boldsymbol{\xi}\|) \quad \forall \mathbf{x} \in \mathcal{D}, \tag{5}$$

then a homogeneous random field $H(\mathbf{x})$ is called *isotropic*. For numerical computations it is useful to represent a continuous random field $H(\mathbf{x})$ in terms of discrete random variables c_k; $k = 1 \ldots \infty$ (Ghanem and Spanos, 1991, Brenner and Bucher, 1995):

$$H(\mathbf{x}) = \sum_{k=1}^{\infty} c_k \phi_k(\mathbf{x}), \quad \mathbf{x} \in \mathcal{D} \subset \mathbb{R}^n; c_k, \phi_k \in \mathbb{R}. \tag{6}$$

The functions $\phi_k(\mathbf{x})$ are deterministic spatial shape functions which are usually chosen to represent an orthonormal basis on $\mathcal{D}$. The random coefficients c_k can be made uncorrelated, which is an extension of orthogonality into the random variable case.

This representation is usually called *Karhunen–Loève Expansion*. It is based on the following decomposition of the covariance function:

$$C_{HH}(\mathbf{x}, \mathbf{y}) = \sum_{k=1}^{\infty} \lambda_k \phi_k(\mathbf{x}) \phi_k(\mathbf{y}), \tag{7}$$

in which λ_k and $\phi_k(\mathbf{x})$ are the eigenvalues and eigenfunctions, respectively. These are solutions to the integral equation

$$\int_{\mathcal{D}} C_{HH}(\mathbf{x}, \mathbf{y}) \phi_k(\mathbf{x}) \mathrm{d}\mathbf{x} = \lambda_k \phi_k(\mathbf{y}). \tag{8}$$

Mathematically, Equation (8) is an integral equation of the second kind.

In most Finite-Element applications the random field $H(\mathbf{x})$ is discretized right from the start as

$$H_i = H(\mathbf{x_i}); \quad i = 1 \ldots N. \tag{9}$$

A spectral representation for the discretized random field is then obtained by

$$H_i = \sum_{k=1}^{N} \phi_k(\mathbf{x_i}) c_k = \sum_{k=1}^{N} \phi_{ik} c_k. \tag{10}$$

Obviously, this is a matrix-vector multiplication

$$\mathbf{H} = \mathbf{\Phi c}. \tag{11}$$

The orthogonality condition for the columns of $\mathbf{\Phi}$ becomes

$$\mathbf{\Phi}^T \mathbf{\Phi} = \mathbf{I} \tag{12}$$

and the covariance matrix of the components of the coefficient vector $\mathbf{c}$ is

$$\mathbf{C_{cc}} = \mathrm{diag}(\sigma_{c_k}^2). \tag{13}$$

Both conditions can be met if the columns $\boldsymbol{\phi}_k$ of the matrix $\mathbf{\Phi}$ solve the following eigenvalue problem:

$$\mathbf{C_{HH}}\boldsymbol{\phi}_k = \sigma_{c_k}^2 \boldsymbol{\phi}_k; \quad k = 1 \ldots N. \tag{14}$$

Statistically, the Karhunen–Loève expansion is equivalent to a representation of the random field by means of a Principal Component Analysis (PCA).

There are engineering applications in which the values of a structural property are known (e.g. from measurements) in certain selected locations. In geotechnical applications this may be a specific soil property which can be determined through bore holes. Between these locations, however, a random variability is assumed. The strategy to deal with this relies on a regression approach. First we assume that the structural property under consideration without any measurements can be modeled by a zero mean random field $H(\mathbf{x})$. This field is modified into $\hat{H}(\mathbf{x})$ by taking into account the additional knowledge.

Assume that the values of the random field $H(\mathbf{x})$ are known at the locations $\mathbf{x}_k,\ k = 1 \ldots m$. We then write a stochastic interpolation for the conditional random field:

$$\hat{H}(\mathbf{x}_i) = a(\mathbf{x}) + \sum_{k=1}^{m} b_k(\mathbf{x}) H(\mathbf{x}_k) \tag{15}$$

in which $a(\mathbf{x})$ and $b_k(\mathbf{x})$ are random interpolating functions whose statistics have yet to be determined. They are chosen to make the mean value of the difference between the random field and the conditional field zero, i.e. $\mathbf{E}[\hat{H}(\mathbf{x}) - H(\mathbf{x})] = 0$ and to minimize the variance of the difference, i.e. $\mathbf{E}[(\hat{H}(\mathbf{x}) - H(\mathbf{x}))^2] \to \mathrm{Min}$.

Carrying out the analysis we obtain an expression for the mean value of the conditional random field.

$$\bar{\hat{H}}(\mathbf{x}) = \left[\ \mathbf{C}_{HH}(\mathbf{x}, \mathbf{x}_1)\ \ \mathbf{C}_{HH}(\mathbf{x}, \mathbf{x}_2)\ \ \ldots\ \ \mathbf{C}_{HH}(\mathbf{x}, \mathbf{x}_m)\ \right] \mathbf{C}_{HH}^{-1} \begin{bmatrix} H(\mathbf{x}_1) \\ H(\mathbf{x}_2) \\ \vdots \\ H(\mathbf{x}_m) \end{bmatrix}. \tag{16}$$

In this equation, the matrix $\mathbf{C}_{HH}$ denotes the covariance matrix of the random field $H(\mathbf{x})$ at the locations of the measurements. The covariance matrix of the conditional random field is given by

$$\hat{\mathbf{C}}(\mathbf{x}, \mathbf{y}) = \mathbf{C}(\mathbf{x}, \mathbf{y}) - \left[\ \mathbf{C}_{HH}(\mathbf{x}, \mathbf{x}_1)\ \ \mathbf{C}_{HH}(\mathbf{x}, \mathbf{x}_2)\ \ \ldots\ \ \mathbf{C}_{HH}(\mathbf{x}, \mathbf{x}_m)\ \right] \mathbf{C}_{HH}^{-1} \begin{bmatrix} \mathbf{C}_{HH}(\mathbf{y}, \mathbf{x}_1) \\ \mathbf{C}_{HH}(\mathbf{y}, \mathbf{x}_2) \\ \vdots \\ \mathbf{C}_{HH}(\mathbf{y}, \mathbf{x}_m) \end{bmatrix}. \tag{17}$$

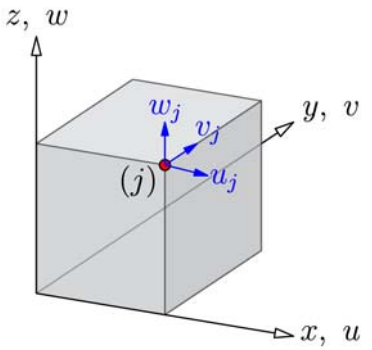

Fig. 2. Volume element with nodal displacements.

2. Stochastic Finite Element Formulation

As discussed earlier, the element stiffness matrix $\mathbf{K}^e$ relates the nodal forces $\mathbf{F}^e$ to the nodal displacements $\mathbf{U}^e$:

$$\mathbf{F}^e = \mathbf{K}^e \mathbf{U}^e \tag{18}$$

in which, for the element with m^e nodes (j); $j = 1 \ldots m^e$ as sketched in Figure 2:

$$\mathbf{F}^e = \left[(f_{xj}, f_{yj}, f_{zj}); j = 1 \ldots m^e\right]^T; \quad \mathbf{U}^e = \left[(u_j, v_j, w_j; j = 1 \ldots m^e\right]^T. \tag{19}$$

Based on the principle of virtual work, the element stiffness matrix for a linear material law (assuming geometrical linearity as well) is obtained as

$$\mathbf{K}^e = \int_{V^e} \mathbf{B}^T(x, y)\mathbf{D}(x, y)\mathbf{B}(x, y) dV^e. \tag{20}$$

Typically, the strain interpolation matrix $\mathbf{B}(x, y)$ is chosen in polynomial form, i.e.

$$\mathbf{B}(x, y) = \sum_{k+l \le r} \sum \mathbf{B}_{kl} x^k y^l; \quad k, l, r \ge 0. \tag{21}$$

In this equation, $\mathbf{B}_{kl}$ are constant matrices. In fact, for the CST element shown above there is only one such matrix, i.e. $\mathbf{B}_{00}$. Assuming that the system randomness is described by a random elastic modulus $E(x, y)$, the elasticity matrix $\mathbf{D}(x, y)$ can be written as

$$\mathbf{D}(x, y) = \mathbf{D}_0 E(x, y). \tag{22}$$

Using the polynomial form of $\mathbf{B}(x, y)$, the element stiffness matrix finally becomes

$$\mathbf{K}^e = \sum_{k+l \le r} \sum \sum_{m+n \le r} \sum \mathbf{B}_{kl}^T \mathbf{D}_0 \mathbf{B}_{mn} \int_{V^e} E(x, y) x^k y^l x^m y^n \, \mathrm{d}V^e. \tag{23}$$

The last term in this equation is a so-called *weighted integral* of the random field $E(x, y)$.

$$X_{klmn}^e = \int_{V^e} E(x, y) x^k y^l x^m y^n \, \mathrm{d}V^e. \tag{24}$$

Using this representation, it is possible to achieve a description of the random variation of the element stiffness matrix in terms of the mean values and the covariance matrix of the weighted integrals.

Due to the numerical rather than analytical integration procedures as utilized in FE analysis, this weighted integral is represented by linear combinations of the values R_j; $j = 1 \ldots n$ of the random field at discrete integration points.

The global stiffness matrix is then assembled by applying standard FE techniques into the form

$$\mathbf{K} = \sum_{j=1}^{n} \mathbf{K}_j R_j, \tag{25}$$

which can be used as a starting point for a perturbation analysis with respect to the discretized random field R_j.

The general situation of a SFE analysis in nonlinear dynamics generally requires the solution of the following matrix-vector equation

$$\mathbf{M}\ddot{\mathbf{x}} + \mathbf{C}\dot{\mathbf{x}} + \mathbf{r}(\mathbf{x}) = \mathbf{f}(t). \tag{26}$$

In Equation (26), $\mathbf{M}$ is the mass matrix, $\mathbf{C}$ is the damping matrix, $\mathbf{x}$ denotes the vector of nodal displacements, $\mathbf{r}(\mathbf{x})$ is the vector of restoring forces depending nonlinearly on the nodal displacements, and $\mathbf{f}(t)$ is the applied load.

Within the FE concept, the restoring force vector $\mathbf{r}(\mathbf{x})$ is assembled from corresponding element forces, e.g. based on the principle of virtual work in the form

$$\mathbf{r}(\mathbf{x})\delta\mathbf{x}_e = \int_{V_e} \sigma_e(\epsilon)\delta\epsilon_e dV_e. \tag{27}$$

In Equation (27), the subscript e refers to a particular element. Obviously, this equation implies that the randomness of the material properties immediately affects the calculated restoring forces due to the integration over the volume of the element. Consequently any randomness of these material data will be reflected in the restoring forces as well as the tangential stiffness matrix $\mathbf{K}_T$ derived from them.

Utilizing a linearization approach at element level, classical SFE-methods as outlined above can be applied.

3. Perturbation Approach

For static problems, the linear finite element equations are

$$\mathbf{K}\mathbf{u} = \mathbf{F}, \tag{28}$$

where $\mathbf{K}$ is the stiffness matrix, $\mathbf{u}$ is the nodal displacement vector and $\mathbf{F}$ is the nodal force vector. In the following we will assume that only the stiffness matrix involves randomness, i.e. the Young's modulus $E(\mathbf{x})$ is described as

$$E(\mathbf{x}) = \bar{E}(1 + \varepsilon f(\mathbf{x})) \tag{29}$$

with $\bar{E}$ and ε as the mean and the coefficient of variation of the Young's modulus, respectively, and $f(\mathbf{x})$ as a zero-mean unit random field. Utilizing the stochastic finite element method the random field is discretized by a set of n zero-mean unit random variables R_j with covariances $Cov[R_j, R_k]$ $(j, k = 1, \ldots, n)$. In case of small to moderate coefficients of variation ε of the Young's modulus a

first-order perturbation approach suffices to render accurate second-moment results. Therewith, the nodal displacements can be written as

$$\mathbf{u} = \bar{\mathbf{u}} + \varepsilon \bar{\mathbf{K}}^{-1} \sum_{j=1}^{n} \left. \frac{\partial \mathbf{K}}{\partial R_j} \right|_{\mu_j} R_j \bar{\mathbf{u}}, \tag{30}$$

whereby $\bar{\mathbf{K}}$ and $\bar{\mathbf{u}}$ are the stiffness matrix and the nodal displacement vector evaluated at the means $\mu_j = 0$ of the random variables R_j. Taking expectations, the mean and the covariance of the nodal displacements are given by

$$E[\mathbf{u}] = \bar{\mathbf{u}} \tag{31}$$

and

$$Cov[\mathbf{u}, \mathbf{u}] = \varepsilon^2 \bar{\mathbf{K}}^{-1} \sum_{j=1}^{n} \sum_{k=1}^{n} \left. \frac{\partial \mathbf{K}}{\partial R_j} \right|_{\mu_j} \bar{\mathbf{u}} \bar{\mathbf{u}}^T \left. \frac{\partial \mathbf{K}}{\partial R_k} \right|_{\mu_k}^{T} Cov[R_j, R_k] \bar{\mathbf{K}}^{-T}, \tag{32}$$

respectively.

To include measured dynamic responses in the random field description – and therewith the nodal displacements – the generalized eigenvalue problem

$$(-\mathbf{M}\lambda_i + \mathbf{K})\,\mathbf{e}_i = \mathbf{0} \tag{33}$$

has to be solved, with $\mathbf{M}$ denoting the (deterministic) stiffness matrix, and λ_i and $\mathbf{e}_i$ the i-th eigenvalue and eigenvector, respectively. Expressing the eigenvalues by their Rayleigh coefficients

$$\lambda_i = \frac{\mathbf{e}_i^T \mathbf{K} \mathbf{e}_i}{\mathbf{e}_i^T \mathbf{M} \mathbf{e}_i} \tag{34}$$

and applying again a first-order perturbation approach, the random eigenvalues λ_i can be expressed as a linear combination of the random variables R_j, i.e.

$$\lambda_i = \bar{\lambda}_i + \varepsilon \sum_{j=1}^{n} \gamma_{ij} R_j = \bar{\lambda}_i + \varepsilon \sum_{j=1}^{n} \frac{1}{\bar{\mathbf{e}}_i^T \mathbf{M} \bar{\mathbf{e}}_i} \bar{\mathbf{e}}_i^T \left. \frac{\partial \mathbf{K}}{\partial R_j} \right|_{\mu_j} \bar{\mathbf{e}}_i R_j, \tag{35}$$

where $\bar{\mathbf{e}}_i$ are the eigenvectors evaluated at $\mu_j = 0$. Given m identified frequencies ω_i ($\lambda_i = \omega_i^2$), this information can be included in the random field description by transforming the random variables R_j such that they are conditional on the set of measurements $\mathbf{s} = [s_1, s_2, \ldots, s_m]$, whereby $s_i = \lambda_i - \bar{\lambda}_i$. Consequently, also the nodal displacements are conditional on the measurements $\mathbf{s}$, i.e. the conditional mean and covariance are

$$E[\mathbf{u}|\mathbf{s}] = \bar{\mathbf{u}} + \varepsilon \bar{\mathbf{K}}^{-1} \sum_{j=1}^{n} \left. \frac{\partial \mathbf{K}}{\partial R_j} \right|_{\mu_j} E[R_j|\mathbf{s}] \bar{\mathbf{u}} \tag{36}$$

and

$$Cov[\mathbf{u}, \mathbf{u}|\mathbf{s}] = \varepsilon^2 \bar{\mathbf{K}}^{-1} \sum_{j=1}^{n} \sum_{k=1}^{n} \left. \frac{\partial \mathbf{K}}{\partial R_j} \right|_{\mu_j} \bar{\mathbf{u}} \bar{\mathbf{u}}^T \left. \frac{\partial \mathbf{K}}{\partial R_k} \right|_{\mu_k}^{T} Cov[R_j, R_k|\mathbf{s}] \bar{\mathbf{K}}^{-T}. \tag{37}$$

4. Random Fields Conditional on Dynamic Measurements

4.1. *Formulation*

As can be seen from Equation (35), the random eigenvalues can be expressed as a linear combination of the random variables R_j with coefficients γ_{ij}. Constructing a new set of random variables $\mathbf{Q}$ by the transformation

$$\mathbf{Q} = \left[\boldsymbol{\gamma}_1, \boldsymbol{\gamma}_2, \ldots, \boldsymbol{\gamma}_n\right]^T \mathbf{R} = \boldsymbol{\Gamma}^T \mathbf{R}, \tag{38}$$

whereby the transformation vectors $\boldsymbol{\gamma}_i$ are defined as $\boldsymbol{\gamma}_i = [\gamma_{i1}, \gamma_{i2}, \ldots, \gamma_{in}]$, the mean and covariance of $\mathbf{Q}$ are

$$E[\mathbf{Q}] = \boldsymbol{\Gamma}^T E[\mathbf{R}] \tag{39}$$

and

$$Cov[\mathbf{Q}, \mathbf{Q}] = \boldsymbol{\Gamma}^T Cov[\mathbf{R}, \mathbf{R}]\, \boldsymbol{\Gamma}, \tag{40}$$

respectively. Given a set of m measurements $\mathbf{s}$, these measurements can be interpreted as a realization of the random vector $\mathbf{S} = [Q_1, Q_2, \ldots, Q_m]$. To include the measurement information in the statistical description of the random field, a conditional random field is defined with mean

$$E[Q_j|\mathbf{s}] = E[Q_j] + Cov[Q_j, \mathbf{S}]\big(Cov[\mathbf{S}, \mathbf{S}]\big)^{-1}\big(\mathbf{s} - E[\mathbf{S}]\big) \tag{41}$$

and covariance

$$Cov[Q_j, Q_k|\mathbf{s}] = Cov[Q_j, Q_k] - Cov[Q_j, \mathbf{S}]\big(Cov[\mathbf{S}, \mathbf{S}]\big)^{-1} Cov[\mathbf{S}, Q_k] \tag{42}$$

that possesses the desired properties (Ditlevsen, 1991). In other words, the random field described by Equations (41) and (42) is conditional on complete agreement with the measurements $\mathbf{s}$ made. The conditional mean and covariance of the original random variables $\mathbf{R}$ – as required by Equations (36) and (37) – are given by

$$E[\mathbf{R}|\mathbf{s}] = \boldsymbol{\Gamma}^{-T} E[\mathbf{Q}|\mathbf{s}] \tag{43}$$

and

$$Cov[\mathbf{R}, \mathbf{R}|\mathbf{s}] = \boldsymbol{\Gamma}^{-T} Cov[\mathbf{Q}, \mathbf{Q}|\mathbf{s}]\, \boldsymbol{\Gamma}^{-1}, \tag{44}$$

respectively.

4.2. *Numerical Example: Plate Structure*

As a numerical example a plate structure of size $4l$ by $2l$ ($l = 1.25$ m) with thickness $t = 0.25$ m is investigated (see Figure 3). Young's modulus $E = 30.0$ GPa, Poisson's ratio $\nu = 0.16$, correlation length $l_c = 1.0$ m, coefficient of variation $\varepsilon = 0.1$, mass density $\varrho = 2500$ kg/m^3, $p(x, y) = 1.6$ MPa.

It is assumed that a set of natural frequencies ω_i is measured (cf. Table 1) for one particular realization of the random field as shown in Figure 4. The unconditional mean and standard deviation of the vertical deflection under the given static load are shown in Figures 5 and 6, respectively. By including the measurements of the two lowest natural frequencies, the standard deviation of the deflection is considerably reduced as shown in Figure 7. As shown in Macke and Bucher (2000), the

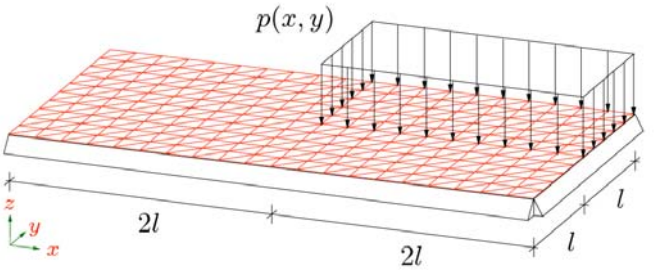

Fig. 3. Plate structure.

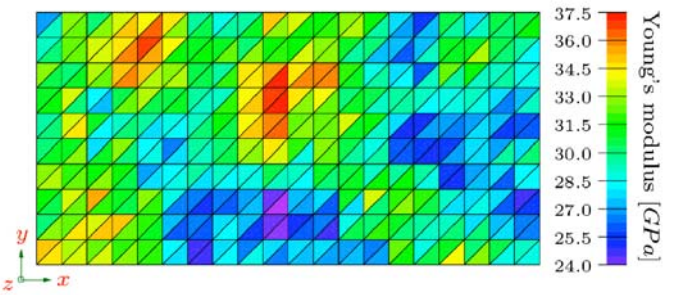

Fig. 4. Realization of random field.

Table 1. Mean and measured frequencies.

i	$\bar{\omega}_i$	ω_i
1	499	504
2	797	796
3	1290	1294
4	1686	1694
5	1976	1979
6	1976	1993
7	2457	2472

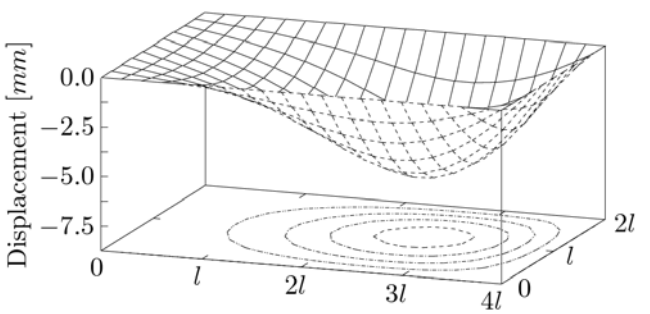

Fig. 5. Mean displacement $\bar{\mathbf{u}}$.

effect of including additional frequency measurement on further reduction of the standard deviation is very small.

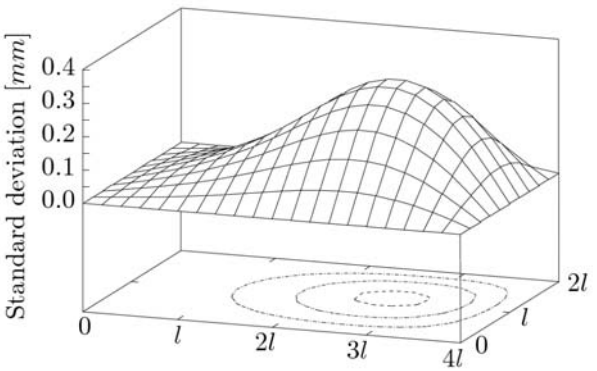

Fig. 6. Initial standard deviation.

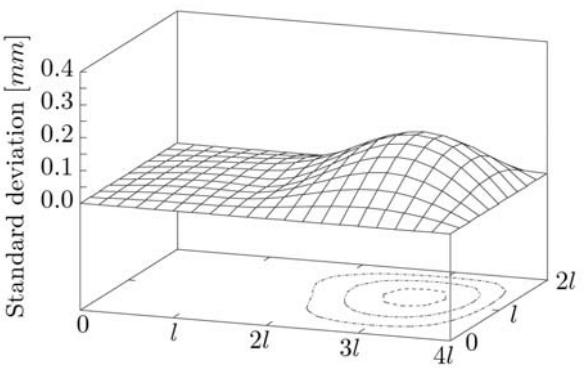

Fig. 7. Conditional standard deviation.

5. Dynamic Stability Analysis

5.1. *Nonlinear Stability Analysis*

The equation of motion of a geometrically nonlinear structural model is given by

$$\mathbf{M}\ddot{\mathbf{x}} + \mathbf{r}(\mathbf{x}, \dot{\mathbf{x}}) = \mathbf{f}(t). \tag{45}$$

For neighboring trajectories, the tangential equation of motion may be utilized to describe temporal evolution of the difference $\mathbf{y}(t)$

$$\mathbf{M}\ddot{\mathbf{y}} + \mathbf{C}\dot{\mathbf{y}} + \mathbf{K}\mathbf{y} = \mathbf{0}. \tag{46}$$

To analyze the dynamic stability behaviour of nonlinear systems an integration of Equation (45) is necessary until stochastic stationarity is reached. In each time step, the tangential stiffness matrix $\mathbf{K}$ has to be determined. With this kind of analysis a criterion for sample stability is developed. In order to speed up explicit time integration, this equation can be projected into a subspace of dimension m as spanned by the eigenvectors of the undamped system corresponding to the m smallest natural frequencies (Bucher, 2001). These eigenvectors are the solutions to

$$\left(\mathbf{K}\left(\mathbf{x}_{\text{stat}}\right) - \omega_i^2 \mathbf{M}\right) \mathbf{\Phi} = 0; \quad i = 1 \ldots m \tag{47}$$

In this equation, $\mathbf{x}_{\text{stat}}$ is chosen to be the displacement solution of Equation (45) under static loading conditions. The mode shapes are assumed to be mass normalized. A transformation $\mathbf{x} = \mathbf{\Phi}\,\mathbf{v}$ and a multiplication of Equation (45) with $\mathbf{\Phi}^T$ represents a projection of the differential equation of motion for the reference solution into the subspace of dimension m as spanned by the eigenvectors:

$$\ddot{\mathbf{v}} + \mathbf{\Phi}^T \mathbf{r}(\mathbf{x}, \dot{\mathbf{x}}) = \mathbf{\Phi}^T \mathbf{f}. \tag{48}$$

The integration of Equation (48) by the central difference method (Bathe, 1996) requires a minimal time step.

The time integration in the subspace and the computing of the restoring forces on the full system causes the following problem: If the start displacement or velocity vector of the time integration is not zero, for example by static loading, the projection of this vectors into the subspace is an optimiziation problem caused by the higher number of variables in the full space. By using a least square approach:

$$\mathbf{v} = \mathbf{\Phi}^{-1}\mathbf{x}; \quad \mathbf{\Phi}^{-1} = \left(\mathbf{\Phi}^T\mathbf{\Phi}\right)\mathbf{\Phi}^T \tag{49}$$

this projection is optimal approximated, but not suitable for a subspace spanned by a small number of eigenvectors. A possibility to handle this, is to start the time integration in the subspace with a displacement and velocity vector equal to zero. The start vectors have to be saved in the full system and the restoring force vector has to be computed by addition of the start and the time integration vectors:

$$\mathbf{r}(\mathbf{x}, \dot{\mathbf{x}}) = \mathbf{r}(\mathbf{x}_{\text{start}} + \mathbf{\Phi}\mathbf{v}, \dot{\mathbf{x}}_{\text{start}} + \mathbf{\Phi}\dot{\mathbf{v}});$$

$$\mathbf{v}(t=0) = \dot{\mathbf{v}}(t=0) = \mathbf{0}. \tag{50}$$

In the investigated cases the start vector $\mathbf{x}_{\text{start}}$ is the static displacement vector, the start velocities are assumed to be vanished.

To analyze the stability behaviour of the reference solution $\mathbf{x}_0(t)$, the long-term behavior of the neighboring motion (Equation (46)) is investigated. To reduce the dimension of the equation system, this equation can be projected into the same or a smaller subspace as Equation (48). Transformed into the state space description we obtain:

$$\dot{\mathbf{z}} = \begin{bmatrix} \mathbf{0} & \mathbf{I} \\ -\mathbf{\Phi}^T\mathbf{K}\mathbf{\Phi} & -\mathbf{\Phi}^T\mathbf{C}\mathbf{\Phi} \end{bmatrix} \mathbf{z} = \mathbf{A}[\mathbf{x}_0(t)]\mathbf{z} \tag{51}$$

From this equation, the Lyapunov exponent λ can be determined by a limiting process:

$$\lambda(\mathbf{x}_0, \mathbf{s}) = \lim_{t\to\infty} \frac{1}{t} \log ||\mathbf{\Theta}(\mathbf{x}_0, t)\mathbf{s}|| \tag{52}$$

in which $\mathbf{s}$ is an arbitrary unit vector. In Equation (52), $\mathbf{\Theta}(\mathbf{x}_0, t)$ is the transition matrix from time 0 to t associated with Equation (51). Based on the multiplicative ergodic theorem (e.g. Arnold and Imkeller, 1994) the Lyapunov exponent can also be calculated as an expected value:

$$\lambda(\mathbf{x}_0, \mathbf{s}) = E\left[\frac{d}{dt} \log ||\mathbf{\Theta}(\mathbf{x}_0, t)\mathbf{s}||\right]. \tag{53}$$

In the current investigation, the norm $||\mathbf{\Theta}(\mathbf{x}_0, t)\mathbf{s}||$ is expressed in terms of

$$\|\mathbf{\Theta}(\mathbf{x}_0, t)\mathbf{s}\| \leq \|\mathbf{\Theta}(\mathbf{x}_0, t)\| \cdot \|\mathbf{s}\| = \|\mathbf{\Theta}(\mathbf{x}_0, t)\|. \tag{54}$$

Finally, this result is used in calculating the Lyapunov exponent according to Equation (52) by using a matrix norm equal to the eigenvalue $\mu_{\max}$ of $\mathbf{\Theta}(\mathbf{x}_0, t)$ with the maximum absolute value. The time domain t has to be taken large enough that the Lyapunov exponent convergences to a stationary value. For the statistical estimation of the convergence of the Lyapunov exponent, Equation (53) is suitable.

5.2. *Linear Stability Analysis*

The Lyapunov exponent for the stability of the second moments of a linearized reference solution can be determined by the Itô analysis. The nonlinear stiffness matrix in Equation (46) can be expanded into an asymptotic series with respect to a static loading condition. Under the assumption that the fluctuating part is small enough this series can be truncated after the linear term:

$$\mathbf{M}\ddot{\mathbf{y}} + \mathbf{C}\dot{\mathbf{y}} + (\mathbf{K}(\mathbf{x}_{\text{stat}}) + \mathbf{f}(t)\mathbf{K}_1)\,\mathbf{y} = \mathbf{0}. \tag{55}$$

This equation of motion is projected into a subspace of dimension m and then transformed into its state space description analogous to Equation (51):

$$\dot{\mathbf{z}} = [\mathbf{A} + \mathbf{B}\mathbf{f}(t)]\,\mathbf{z}, \tag{56}$$

where the coefficient matrices $\mathbf{A}$ and $\mathbf{B}$ are constant. The fluctuating part of the loading function is assumed to be Gaussian white noise. Then Equation (56) represents a first order stochastic differential equation. For this system the Lyapunov exponent λ_2 for the second moments can be easily derived by applying the Itô calculus (e.g. Soong and Grigoriu, 1992; Lin and Cai, 1995).

The Lyapunov exponents for almost sure stability can be approximated for linear SDOF-systems analytically (Lin and Cai, 1995):

$$\lambda = -\zeta_0\omega_0 + \frac{\pi S_{ff}\omega_0^2}{4}, \tag{57}$$

where ω_0 is the eigenfrequency, ζ_0 is the modal damping ratio and S_{ff} is the power spectral density of the white noise excitation. The Lyapunov exponent λ_2 for the second moments can be calculated with

$$\lambda_2 = -2\zeta_0\omega_0 + \pi S_{ff}\omega_0^2. \tag{58}$$

By exploiting this, the Lyapunov exponent for the samples can be appproximated from the second moment exponent according to

$$\lambda = \frac{\lambda_2}{4} - \frac{\zeta_0\omega_0}{2}. \tag{59}$$

This equation can also be applied on MDOF-systems, it should be mentioned that the term $-\zeta_0\omega_0$ corresponds then to the Lyapunov exponent of the system without random parametric excitation.

5.3. *Reliability Investigation of a Shell Structure*

A cylindrical panel was considered, which is mentioned e.g. in Krätzig (1989) and Schorling and Bucher (1999). The assumed structure is shown in Figure 8. The geometrical and the material proberties were given as: radius $R = 83.33$ m, the half width and heigth $a = 5$ m, the thickness $h = 0.1$ m, the Young's modulus $E = 3.4 \times 10^{10}$ N/m^2, the mass density $\rho = 3400$ kg/m^3 and the Poisson's ratio $\mu = 0.2$. The constant load factor is $P = 1000$ N/m.

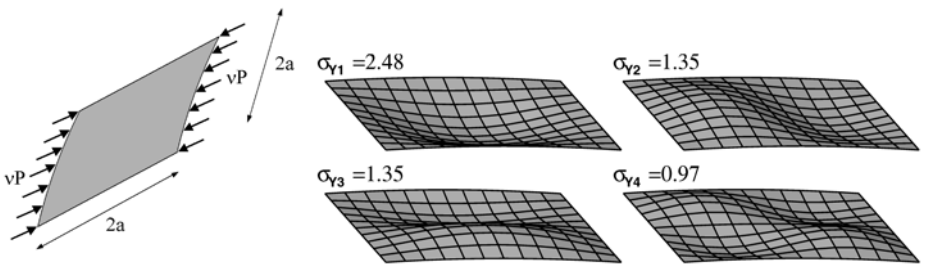

Fig. 8. Nonlinear cylindrical shell structure with associated weighted imperfection shapes.

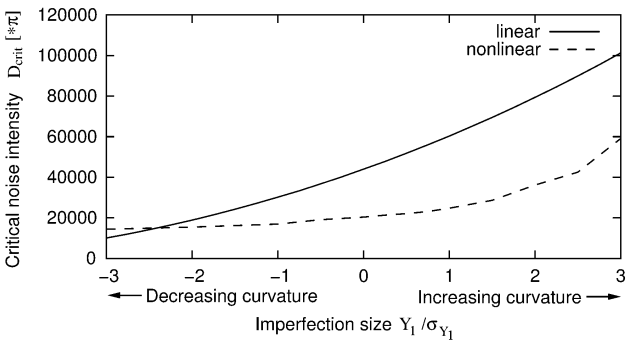

Fig. 9. Stability boundaries vs. imperfection size.

The structure is discretized with 7×7 nodes and meshed with geometrically nonlinear 9-node shell elements. At a static load factor of $\nu_{\text{crit}} = 16825$ the structure reaches an unstable state (Krätzig, 1989: $\nu_{\text{crit}} = 15120$; Schorling and Bucher, 1999: $\nu_{\text{crit}} = 16200$). The static load is assumed to be $P_0 = 0.85\nu_{\text{crit}}P$. The fluctuating load is considered as $P_{\text{fluct}} = \ell f(t)P$, where $f(t)$ is the unit white noise process and ℓ is the load factor. The damping is assumed as modal damping with the damping ratio $\zeta_k = 0.02$ for all modes.

The geometrical imperfections are considered in terms of radial deviations from the perfect panel surface and are modelled as a conditional Gaussian random field. The mean is assumed as zero and the standard deviation as $\sigma = 10^{-3}$ m. The correlation length of the exponential correlation function is considered with $l_H = 10$ m. The imperfection shapes are obtained by the decomposition of the covariance matrix according to Equation (14). The first four imperfection shapes are shown in Figure 8 as well. The corresponding standard deviations σ_{Yi} in uncorrelated normal space are indicated in the figure. The first shape is very similar to the buckling shape.

The structure was investigated by using the Itô analysis and it was found that only the first imperfection shape has a major influence on the stability behaviour. The critical noise intensity of the perfect system was obtained as $D_{0_{\text{crit}}} = 92000\pi$ with the linear and $D_{0_{\text{crit}}} = 20000\pi$ with the nonlinear method by averaging 20 simulations with 10^5 time steps. The nonlinear analysis uses a modal subspace spanned by 12 of the 213 eigenmodes with a critical time step of $\Delta t = 6.3 \cdot 10^{-3}$ s. The investigation of the first imperfection shape obtained by nonlinear analysis show observable deviations from the linear results. This points out that the nonlinearities of this structure have a higher influence as compared to the previous example. The obtained stability boundaries depending on the imperfection size are displayed in Figure 9 for the linear and the nonlinear analysis.

The failure probability for this one dimensional problem can be obtained analytical from the stability boundaries and is shown in Figure 10 depending on the noise intensity for both methods. It

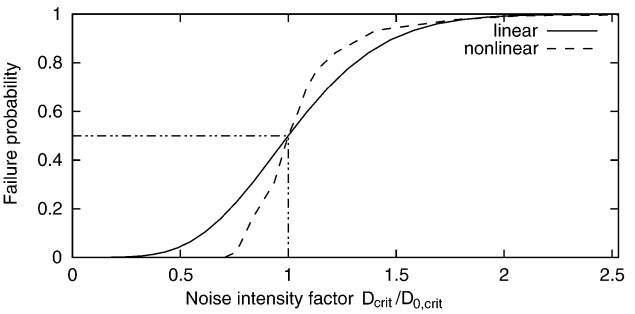

Fig. 10. Failure probabilities for both methods.

Table 2. Critical static and dynamic loads.

Model	ν_{crit}	$D_{0_{\text{crit}}}$ $\nu = 0.85\nu_{\text{crit}}$	$D_{0_{\text{crit}}}$ $\nu = 0.85\nu_{\text{crit},7\times7}$
7×7	16825	91736π	91736π
11×13	15968	43946π	32116π
25×25	15744	32353π	13854π

is to be seen in the picture, that a sufficient approximation of the nonlinear probability graph is not possible with the linear method.

Furthermore the discretisation influence on the stability boundaries was investigated on the perfect panel. Additional to the 7×7 node model, systems modeled with 11×13 (Schorling and Bucher, 1999) and 25×25 nodes and meshed with geometrically nonlinear 9-node shell elements were analyzed. The critical static buckling loads are shown in Table 2. The dynamic stability boundaries are obtained by using the linear Itô analysis under considering the static load first with $0.85\nu_{\text{crit}}$ of the same model. This leads to different static loads. To obtain the stability boundaries by a constant static load this load was assumed as $0.85\nu_{\text{crit}}$ of the 7×7 node model. The results are shown additional in Table 2. It is to be seen that the influence of the discretization on the critical noise intensity is much higher than on the static buckling load.

The nonlinear method was not applicable for the 11×13 and 25×25 node models, caused by the hugh numerical effort. Simulations with the 11×13 node model by using a modal reduction from 657 eigenmodes to 33 eigenmodes (the critical time step is then $3.4 \cdot 10^{-3}$ s) did not lead to sufficient results. The Lyapunov exponent did not converge to a stationary value, caused be the to short time window of the simulations, limited by the available computer capacities.

References

Arnold, L. and P. Imkeller (1994). Fürstenberg–Khasminskii formulas for Lyapunov exponents via anticipative calculus. Technical Report Report Nr. 317, Institut für dynamische Systeme, University of Bremen.

Bathe, K.-J. (1996). *Finite Element Procedures*. Englewood Cliffs: Prentice Hall.

Brenner, C. E. and C. Bucher (1995). A contribution to the SFE-based reliability assessment of nonlinear structures under dynamic loading. *Probabilistic Engineering Mechanics* **10**, 265–273.

Bucher, C. (2001). Stabilization of explicit time integration by modal reduction. In W. A. Wall, K.-U. Bletzinger, and K. Schweizerhof (Eds.), *Proceedings, Trends in Computational Mechancics*. Barcelona: CINME.

Bucher, C., O. Huth, and M. Macke (2003). Accuracy of system identification in the presence of random fields. In A. DerKiureghian, S. Madanat, and J. Pestana (Eds.), *Applications of Statistics and Probability in Civil Engineering*, pp. 427–433. Millpress.

Ditlevsen, O. (1991). Random field interpolation between point by point measures properties. In *Proceedings of 1. Int. Conference on Computational Stochastic Mechanics*, pp. 801–812. Computational Mechanics Publications.

Ghanem, R. and P. D. Spanos (1991). *Stochastic Finite Elements – A Spectral Approach*. New York/Berlin/Heidelberg: Springer.

Krätzig, W. (1989). Eine einheitliche statische und dynamische Stabilitätstheorie für Pfadverfolgungsalgorithmen in der numerischen Festkörpermechanik. *Z. angew. Math. Mech.* **69-7**, 203–213.

Lin, Y.-K. and G.-Q. Cai (1995). *Probabilistic Structural Dynamics*. New York: McGraw-Hill.

Macke, M. and C. Bucher (2000). Conditional random fields for finite elements based on dynamic response. In M. Deville and R. Owens (Eds.), *Proc. 16th IMACS World Congress on Scientific Computation, Applied Mathematics and Simulation*, Lausanne, Switzerland, August 21–25, 2000.

Matthies, H. G. and C. Bucher (1999). Finite Elements for Stochastic Media Problems. *Comput. Methods Appl. Mech. Engrg.* **168**, 3–17.

Matthies, H. G., C. E. Brenner, C. G. Bucher, and C. G. Soares (1997). Uncertainties in Probabilistic Numerical Analysis of Structures and Solids – Stochastic Finite Elements. *Struct. Safety* **19**, 283–336.

Most, T., C. Bucher, and Y. Schorling (2004). Dynamic stability analysis of nonlinear structures with geometrical imperfections under random loading. *Journal of Sound and Vibration* **1–2**(276), 381–400.

Schorling, Y. and C. Bucher (1999). Stochastic stability of structures with random imperfections. In B. F. J. Spencer and E. A. Johnson (Eds.), *Stochastic Structural Dynamics*, pp. 343–348. Rotterdam/Brookfield: Balkema.

Soong, T.-T. and M. Grigoriu (1992). *Random Vibrations of Mechanical and Structural Systems*. Englewood Cliffs: Prentice Hall.